Contrib Mineral Petrol (1998) 133: 122–135

P. Nimis · P. Ulmer

Clinopyroxene geobarometry of magmatic rocks Part 1: An expanded structural geobarometer for anhydrous and hydrous, basic and ultrabasic systems

Received: 20 October 1996 / Accepted: 18 March 1998

Abstract Crystal-structure modeling of experimental Ca-rich clinopyroxenes [Ca + Na > 0.5 apfu; Mg/(Mg + Fe^{2+}) > 0.7] coexisting with basic and ultrabasic melts was utilized for calibration of geobarometers based on unit-cell volume (V_{cell}) vs M1-site volume (V_{M1}). The clinopyroxene database includes over one hundred experiments from literature and sixteen previously unpublished experiments on basanite and picrobasalt starting materials. The coexisting melts span a wide range of petrologically relevant anhydrous and hydrous compositions (from quartz-normative basalt to nephelinite, excluding high-Al basalts and melts coexisting with garnet or melilite) at pressure conditions pertinent to the earth's crust and uppermost mantle (P = 0–24 kbar) in a variety of f_{O_2} conditions (from CCO-buffered to air-buffered) and mineral assemblages (Cpx ± Opx ± Pig ± Ol ± Plag ± Lc ± Ne ± Spl ± Amp ± Ilm). As previously found for near-liquidus products of basaltic melts, the experimental clinopyroxenes follow two distinct trends: (i) at a given P, V_{cell} is linearly and negatively correlated with V_{M1}. This corresponds with the extent of Tschermak-type substitutions, which depends strongly on a_{SiO_2} and a_{CaO}; (ii) for a fixed melt composition, V_{cell} and V_{M1} decrease linearly as P increases, due to a combination of M_1, M_2 and T site exchanges. Despite the *chemical* complexity of these relationships, P could be modeled as a linear function of V_{cell} and V_{M1}. A simplified solution for anhydrous magmas reproduced the experimental pressures with an uncertainty of 1.75 kbar (= 1σ; max. dev. = 5.5 kbar; N = 135). An expanded T-dependent solution capable of recovering the measured pressures of both anhydrous and hydrous experiments with an uncertainty of 1.70 kbar (= 1σ; max. dev. = 5.4 kbar; N = 157) was obtained by correcting unit-cell and M1-site volumes for thermal expansivity and compressibility. The corrected formulation is more resistant to the effects of temperature variations and is therefore recommended. Nevertheless, it requires an independent, accurate estimate of crystallization T. Underestimating T by 20 °C propagates into a 1-kbar increase of calculated P. The applicability of the T-dependent formulation was tested on hydrous ultramafic to gabbroic rocks of the southern Adamello batholith for which P-T evolution could independently be constrained by field observation, petrography and experimentally determined phase relations. The pressure estimates obtained by clinopyroxene structural geobarometry closely matched those predicted by phase equilibria of a picrobasaltic melt parental to the investigated magmatic rocks. To facilitate application of the present geobarometers, both *anhydrous* and *corrected* solutions were implemented as MS-DOS® and UNIX® software programs (CpxBar) designed to permit retrieval of the pressure of crystallization directly from a chemical analysis or from uncorrected unit-cell and M1-site volume X-ray data.

P. Nimis
Dipartimento di Mineralogia e Petrologia,
Università degli Studi di Padova,
C.so Garibaldi 37-35100 Padova, Italy
Fax: +39-49-8272010, e-mail: nimis@dmp.unipd.it

P. Ulmer
Institut für Mineralogie und Petrologie,
ETH Zentrum, CH-8092 Zürich, Switzerland

Editorial responsibility: I.S.E. Carmichael

Introduction

Duhem's theorem shows that for a closed system there are two independent variables under equilibrium condition. An important petrological consequence is that in a magma that crystallizes at depth the composition of any mineral being segregated from the melt is a function of temperature (T), pressure (P) and bulk composition. Because the bulk compositions of natural magmatic systems are usually unknown, any correlation between the composition of a *single* mineral and P-T conditions is generally equivocal.

Despite this limitation, crystal-structure modeling[1] of experimental near-liquidus clinopyroxenes synthesized from basaltic starting materials (Nimis 1995) showed that: (i) cell and M1-site volumes (hereafter V_{cell} and V_{M1}, respectively) decrease linearly as P (and T) increases, irrespective of magma bulk composition, due to a combination of $Ca_{M2}\ Mg_{M1} \rightarrow Na_{M2}Al_{M1}$, $Mg_{M1}Si_T \rightarrow Al_{M1}Al_T$ and $Ca_{M2} \rightarrow Mg_{M2}$ exchanges; (ii) at a given P, the V_{cell}/V_{M1} ratio, which reflects the substitution of Ca-Tschermak's components [e.g. $Mg_{M2}Mg_{M1}(Si_T)_2 \rightarrow Ca_{M2}Ti_{M1}(Al_T)_2$; $Mg_{M2}Mg_{M1}Si_T \rightarrow Ca_{M2}(Fe^{3+}, Al)_{M1}Al_T$], depend on a_{CaO} and a_{SiO_2} in the melt; (iii) despite the *chemical* complexity of these relations, the *structural* response of clinopyroxene to variations in physico-chemical conditions is quite simple, so that pressure can be expressed as a linear function of V_{cell} and V_{M1}. Equation 4 in Nimis (1995) reproduced the experimental pressures with an overall uncertainty of ± 2 kbar (1σ) and was successfully applied to a few suites of natural pyroxenites and megacrysts, for which it yielded geologically consistent estimates (Nimis 1995, 1998; J. Gutmann pers. comm. 1995; V Hurai pers. comm. 1997). Where available, pressure estimates from fluid inclusion studies turned out to be very close to those retrieved by host clinopyroxene geobarometry (V Hurai pers. comm. 1995).

In spite of these intriguing results, the earlier geobarometric calibration and its applicability still suffered from the following shortcomings:

(i) the experimental database included only near-liquidus products. This choice enabled the trends due to changes in physical conditions to be followed at essentially constant melt composition. It thus permitted evaluation of the net effect of pressure, but considerably diminished the number of data usable for calibration ($N = 29$);

(ii) only experiments with basaltic starting materials were utilized. This had the advantage of reducing bulk chemical variations, yet it restricted the applicability of the geobarometer to clinopyroxenes for which a crystallization from melts of strictly basaltic compositions could be demonstrated. In the case of high-pressure cumulates, for which the geobarometer is expected to give the most useful results, this documentation is not straightforward, since no trace of the parent melts can usually be found. Further, evidence exists that many high-pressure ultramafic nodules or megacrysts crystallized from basanitic or hawaiitic melts rather than from basalts (e.g. Knutson and Green 1975; Ellis 1976; Irving 1980);

(iii) only experiments under anhydrous conditions were considered. Although hydrous basic magmas usually crystallize amphibole at low T, the absence of hydrous mineral phases in a cumulate is not sufficient to rule out the presence of a significant amount of water in the parent melt (e.g. Sisson and Grove 1993);

(iv) the crystal chemical behavior of clinopyroxene at low P (< 8 kbar) was poorly constrained due to the paucity of near-liquidus data at such low pressures.

In the present paper we address these deficiencies by using an expanded set of experimental data that is intended to cover a wide range of dry and hydrous melt compositions, from quartz-normative basalt to low-alkali nephelinite to trachybasalt, including sixteen previously unpublished experiments on basanite and picrobasalt.

The literature database

In constructing the literature database we adopted the following standards: (i) for experiments far from the liquidus ($T_{exp} - T_{liq} > 50$ °C), the composition of the coexisting melt must be known and fall within the fields of basalt, trachybasalt, basanite-tephrite, or low-alkali foidite according to the total-alkali-silica (TAS) classification diagram (Fig. 1); (ii) for near-liquidus experiments for which the composition of the coexisting melt is unknown, at least the composition of the starting material must meet the previous criterion; (iii) there must be documentation of achieved equilibrium between the clinopyroxene and the melt; (iv) the composition of the melt or of the starting material must be relevant to petrological purposes. The last point rejects experimental data based on synthetic subsystems, such as CMAS or Fe-free basalt, or doped systems bearing significant fractions of elements that are normally present in trace amounts. An exception was made for a few high-pressure clinopyroxenes bearing small, although non-negligible amounts of rare earth elements ($REE_2O_3 < 2$ wt%; Adam and Green 1995) and Hf ($HfO_2 < 0.6$ wt%; Dunn 1987).

Since the accuracy of crystal-structure simulation depends strongly on the quality of input chemical analysis, it was necessary to check the reliability of the electron microprobe data before appending them to the database. Analyses that showed high standard deviations (≥ 1 wt% absolute) for CaO and Al_2O_3 were rejected. All other chemical analyses were processed with a locally modified version of the program of Papike et al. (1974) to convert oxide weight percentages into atoms per 6-oxygen formula unit (apfu) and compute Fe^{3+}/Fe^{2+} ratios on a charge-balance basis. After Fe^{3+} evaluation, any REE and Hf were added to Ca and Mg, respectively.[2] Then the following restraints were adopted to verify the reliability of the analyses from a crystal

[1]This procedure allows one to calculate with reasonable uncertainties the structural parameters (unit-cell parameters, atomic fractional coordinates, site geometries) of a $C2/c$ pyroxene from a major-oxide chemical analysis without requiring direct X-ray diffraction measurements.

[2]This expedient relies upon steric arguments and is based on the assumption that REE have broadly the same influence as Ca and Hf has the same effect as Mg on the crystal structure of clinopyroxene, as suggested by the similarity of their respective ionic radii (Shannon 1976).

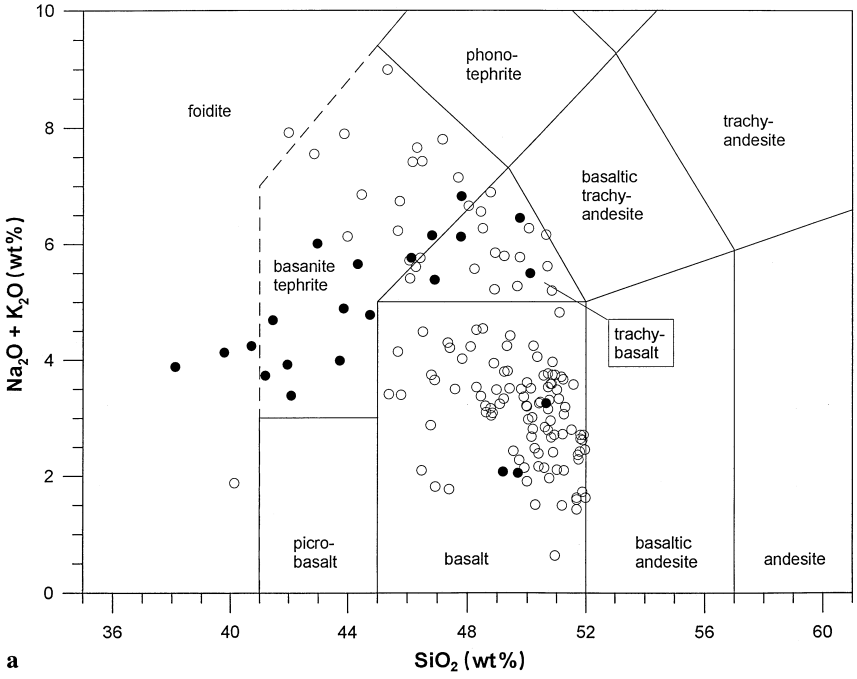

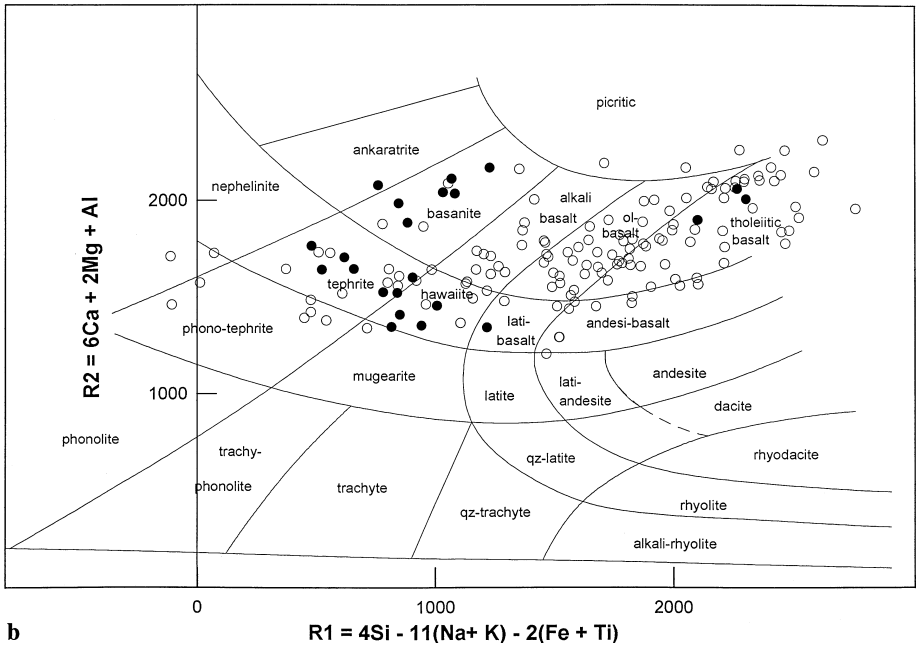

Fig. 1a, b Composition of experimental melts coexisting with clinopyroxenes utilized for geobarometer calibration in the (**a**) TAS (Le Maitre et al. 1989) and (**b**) De La Roche's (De La Roche et al. 1980, modified by Bellieni et al. 1981) classification diagrams. *Filled circles* refer to hydrous experiments. Source of data as in Fig. 2

chemical point of view: (i) the sum of T cations (Si and Al_T) must equal 2.000 ± 0.002 apfu and (ii) the sum of M2 and M1 cations (i.e. Al − (2 − Si) + Ti + Cr + Fe^{3+} + Fe^{2+} + Mn + Mg + Ca + Na) must equal 2.000 ± 0.005 apfu. Cation fractions in both T and M2 + M1 sites were then normalized to 2.000 apfu and utilized as input values for structure modeling. Additionally, only clinopyroxenes with (Ca + Na) > 0.5 apfu and Mg/(Mg + Fe^{2+}) > 0.7 were considered, and in pyroxenes displaying sectors zoning, only compositions referring to sectors (= edges) parallel to the elongation axis were utilized. According to Duncan and Preston (1980), these sectors most likely represent equilibrium compositions. It is worth noting that the supposedly metastable sectors always gave higher residuals in the subsequent statistical analyses. Finally, as noted by Nimis (1995) and corroborated here, the same P-V_{cell}–V_{M1} correlation does not apply to clinopyroxenes from high-alumina basalts[3] or coexisting with gar-

[3]High-alumina basalt has not been formally defined (Le Maitre et al. 1989) and is generally considered as basalt showing higher Al_2O_3 than tholeiite for similar SiO_2 and alkali contents and lower alkali than alkaline basalt. It is regarded here as basalt or trachybasalt showing Al_2O_3 (wt%)/SiO_2 (wt%) > 0.375. This ratio usually corresponds to Al_2O_3 > ca. 18 wt%.

net or melilite. Such pyroxenes were not considered for calibration.

Additional experiments

Sixteen, previously unpublished experimental data were used to extend the compositional range of melts coexisting with clinopyroxene. The experiments cover the range 5 to 20 kbar and 1100–1300 °C, with an additional experiment at 1 bar, and f_{O_2} conditions near the cobalt-cobaltoxide (CCO) equilibrium (Table 1). The high-pressure experiments were performed under H_2O undersaturated conditions. Starting materials for the melting experiments were natural basanitic and picrobasaltic dike rocks from the Northern Calcareous Alps (Austria, basanite) and the southern Adamello (Italy, calc-alkaline picrobasalt) (see caption of Table 1 for details and references).

The high-pressure experiments (5–20 kbar) were performed in end-loaded piston cylinder apparatus. The finely ground rock powders were contained in graphite crucibles sealed in Pt capsules. Standard talc-Pyrex and NaCl-Pyrex assemblies of 14 mm outer diameter were used. The pressure was calibrated against the albite-jadeite-quartz reaction (Johannes et al. 1971) at 600 °C and 16.4 kbar, the quartz-coesite transition (Bose and Ganguly 1995) at 1000 °C and 30.7 kbar, and the orthoferrosilite-fayalite-quartz reaction (Bohlen et al. 1980) at 1000 °C and 14.1 kbar. Temperatures were measured with Pt-Pt_{90} Rh_{10} (type S) thermocouples and controlled to within ±2 °C of the stated value. No correction for the pressure effect on the EMF was applied.

The single 1-bar experiment (PU458) was conducted with the wire-loop technique (Presnall and Brenner. 1974). The powdered starting material was devolatilized over night at 1100 °C and 30–40 mg of the dried powder was sintered on a Pt-wire loop (0.1 mm diameter wire) at 1200 °C for 1 min. The sintered beads were suspended in a vertical quench furnace equipped with a gas-mixing device. The f_{O_2} was controlled with H_2-CO_2 gas mixtures passed into the furnace from below. An f_{O_2} corresponding to the cobalt-cobaltoxide (CCO) buffer was used (−9.82 at 1150 °C). Fe-loss to the Pt-wire was less than 2% relative. Temperatures were measured with Pt - Pt_{90} Rh_{10} thermocouples located within 5 mm of the sample. Temperatures are believed to be accurate to within 2–3 °C and the logf_{O_2} to within 0.1 log-unit.

After termination of the experiment, the samples were embedded in epoxy resin and ground to expose the center of the charges. All phases were identified and measured with either an ARL SEMQ or Cameca SX50 electron microprobe. The following criteria were used to argue in favour of achievement of equilibrium: excepting six clinopyroxenes showing sector-type zoning, crystals coexisting with melt are unzoned, they exhibit idiomorphic shape and their compositions vary systematically with pressure and temperature. The Fe/Mg partitioning between olivine, clinopyroxene, and melt are all within the range of published values. In addition, run durations were quite long from 4 h at 1300 °C to 100 h at 1050 °C. Compositions of clinopyroxene and coexisting melts are given in Table 2.

The final adopted database, inclusive of both literature and additional experiments, covers a wide range of petrologically relevant anhydrous and hydrous melt compositions (Fig. 1) at pressure conditions pertinent to the earth crust and uppermost mantle ($0 \le P \le 24$ kbar) in a variety of f_{O_2} values (from CCO-buffered to air-buffered) and mineral assemblages (Cpx ± Opx ± Pig ± Ol ± Plag ± Lc ± Ne ± Spl ± Amp ± Ilm). Magmas ranging in composition from quartz-normative basalts to nephelinites are represented at all pressures with the however notable exception of high-alumina basalts, while only low-pressure experiments are available for Fe-Ti basalts (N = 9).

An approximate solution for anhydrous basic magmas

The structure of the selected experimental clinopyroxenes were modeled following procedures described in detail by Nimis (1995). A multiple regression in the form $P = a + b \cdot V_{cell} + c \cdot V_{M1}$ based on the experimental database, considering only anhydrous experiments (N = 135), yielded the following geobarometric formulation:

$$P(\text{kbar}) = 771.48(\pm 19.26) - 1.323(\pm 0.051)V_{cell}(\text{Å}^3) - 16.064(\pm 1.228) \cdot V_{M1}(\text{Å}^3) \quad (\sigma = 1.75 \text{ kbar; max. dev.} = 5.5 \text{ kbar; R} = 0.962) \quad (1)$$

It is to be stressed that the variations in V_{cell} or $V_{M!}$ considered here are solely those induced by chemical changes. That is they do not take into account compressibility or thermal expansivity as they would if they were determined by high-P, high-T in situ studies. However, this information is always lost in the natural samples, for which the geobarometer is suited, due to structure relaxation. Using chemistry-structure coefficients reported in Nimis (1995), Eq. 1 can be recast into

Table 1 Experimental conditions and results of the experiments used for the calibration of the clinopyroxene barometer. Starting materials are natural rock powders of a basanite dike (Ulmer et al. 1989; Trommsdorff et al. 1990) with 4.3 wt% H_2O (EJ3-H), the anhydrous equivalent (fired, EJ3-A), and natural rock powders of a calc-alkaline picrobasalt with 2.6 wt% H_2O (RC158; Ulmer 1989) [*ol* olivine, *cpx* clinopyroxene (Ca-rich), *amph* amphibole, *sp* spinel (Cr-rich), *ilm* ilmenite, *cc* calcite, *L* liquid (glass)]

Run #	P (kbar)	T (°C)	Starting material	Time (hours)	Product phases
PU371	20	1300	EJ3-H	3.5	ol, cpx, L
PU372	20	1200	EJ3-H	17.0	ol, cpx, sp, L
PU374	20	1150	EJ3-H	22.0	ol, cpx, amph, L
PU376	20	1100	EJ3-H	65.0	cpx, amph, ilm, L
PU378	15	1200	EJ3-H	46.3	ol, cpx, sp, L
PU380	15	1100	EJ3-H	96.0	ol, cpx, amph, ilm, L
PU400	10	1150	EJ3-H	55.0	ol, cpx, amph, L
PU401	10	1050	EJ3-H	95.3	ol, cpx, amph, cc, L
PU402	10	1100	EJ3-H	70.0	ol, cpx, amph, L
PU403	10	1200	EJ3-H	22.8	ol, cpx, L
PU458	0.001	1150	EJ3-A	72.0	ol, cpx, plag, ilm, L
PU480	5	1150	EJ3-H	46.8	ol, cpx, sp, L
PU483	5	1100	EJ3-H	66.0	ol, cpx, sp, L
P1151	10	1150	RC158	30.0	ol, cpx, sp, L
P1180	10	1180	RC158	25.9	ol, cpx, sp, L
R3	10	1200	RC158	21.5	ol, cpx, L

Table 2 Composition of clinopyroxene (cpx) and coexisting melts (gl) in experiments on basanite and picrobasalt (Table 1). 1 σ standard deviations (in parentheses) on n analyses refer to the last digits. (*HAl* high-alumina sector in sector-zoned clinopyroxene)

Run #	*P* (kbar)	*T* (°C)	Phase analyzed	n	SiO_2	TiO_2	Al_2O_3	Cr_2O_3	FeO	MnO	MgO	NiO	CaO	Na_2O	K_2O	Sum
Basanite runs																
PU371	20	1300	gl	6	39.03(71)	3.48(10)	11.70(34)	0.08(3)	10.30(36)	0.18(3)	12.57(74)	0.01(1)	12.28(30)	2.22(10)	0.92(4)	92.77
			cpx	5	48.62(70)	1.37(17)	9.07(49)	0.25(6)	4.09(23)	0.07(4)	14.67(15)	0.02(2)	20.63(10)	0.85(2)	0.02(2)	99.67
PU372	20	1200	gl	6	38.08(57)	4.10(11)	12.94(23)	0.06(1)	11.99(45)	0.25(4)	11.11(91)	0.01(2)	11.00(17)	2.69(17)	1.27(7)	93.50
			cpx	4	48.02(36)	1.83(11)	9.12(59)	0.10(4)	5.03(27)	0.13(5)	13.71(31)	0.05(5)	20.41(32)	1.11(2)	0.02(1)	99.52
PU374	20	1150	gl	8	39.07(1.21)	3.80(6)	12.53(23)	0.04(2)	11.64(61)	0.20(2)	12.29(54)	0.01(3)	11.72(27)	2.40(17)	1.13(7)	94.82
			cpx	7	48.27(34)	1.73(29)	8.14(35)	0.26(37)	6.18(72)	0.15(4)	13.37(89)	0.02(2)	20.30(29)	0.99(8)	0.03(5)	99.42
PU376	20	1100	gl	8	32.16(2.81)	4.56(56)	10.95(37)	0.01(2)	15.31(1.61)	0.27(3)	8.37(1.49)	0.03(3)	9.46(1.21)	2.58(21)	0.69(8)	84.39
			cpx	8	49.36(59)	1.51(11)	6.23(29)	0.06(2)	6.51(20)	0.14(4)	13.72(16)	0.02(1)	21.02(20)	0.85(2)	0.02(3)	99.44
PU378	15	1200	gl	10	39.02(47)	3.86(6)	13.07(14)	0.03(3)	11.07(26)	0.19(4)	10.12(36)	0.01(2)	11.98(19)	2.58(6)	1.07(4)	92.99
			cpx	7	47.72(53)	2.02(11)	9.42(66)	0.18(8)	2.80(30)	0.11(5)	13.64(21)	0.00(1)	22.03(31)	0.73(6)	0.05(6)	98.70
PU380	15	1100	gl	12	34.92(45)	4.22(23)	12.34(42)	0.02(2)	14.99(66)	0.29(7)	6.95(1.05)	0.02(4)	10.44(96)	2.80(26)	0.81(22)	87.79
			cpx	6	49.19(51)	1.68(18)	6.41(58)	0.07(2)	4.69(34)	0.15(5)	13.60(22)	0.02(2)	21.65(15)	0.74(6)	0.03(3)	98.24
PU400	10	1150	gl	9	40.16(19)	3.93(7)	13.70(18)	0.01(1)	9.55(16)	0.15(2)	8.42(7)	n.a.	11.18(9)	3.16(4)	1.30(4)	91.56
			cpx	8	48.29(30)	1.68(5)	6.51(17)	0.40(7)	4.02(18)	0.10(6)	15.07(24)	n.a.	21.57(34)	0.52(4)	0.03(1)	98.20
PU401	10	1050	gl	11	38.86(52)	3.69(16)	14.83(40)	0.01(1)	9.30(27)	0.27(5)	6.53(42)	n.a.	9.21(9)	3.02(36)	1.11(12)	86.81
			cpx	7	49.89(52)	1.42(16)	4.90(31)	0.07(2)	6.70(25)	0.18(5)	14.12(34)	n.a.	21.22(43)	0.52(4)	0.02(1)	99.04
PU402	10	1100	gl	10	40.66(24)	4.08(9)	15.17(28)	0.01(2)	10.24(25)	0.22(4)	6.62(8)	n.a.	9.52(17)	3.72(6)	1.47(3)	91.70
			cpx	8	49.11(45)	1.71(11)	5.85(41)	0.12(12)	5.71(32)	0.13(6)	13.84(32)	n.a.	21.79(42)	0.56(7)	0.02(1)	98.85
PU403	10	1200	gl	10	38.21(91)	3.42(9)	10.74(28)	0.06(3)	9.50(31)	0.21(3)	8.75(21)	n.a.	12.98(14)	2.49(7)	0.99(2)	87.35
			cpx	6	46.60(68)	2.40(16)	8.72(44)	0.55(11)	3.97(7)	0.07(4)	13.61(24)	n.a.	23.00(9)	0.47(4)	0.01(1)	99.37
PU458	0	1150	gl	2	38.07(1.03)	7.90(25)	12.73(2.52)	0.01(1)	13.97(16)	0.30(2)	6.93(2.51)	n.a.	13.19(1.53)	1.00(14)	0.79(1)	95.83
			cpx HAl	6	43.65(31)	3.94(20)	8.92(53)	0.03(4)	7.38(35)	0.08(3)	11.68(14)	n.a.	23.34(8)	0.23(4)	0.01(1)	99.24
PU480	5	1150	gl	5	38.67(17)	4.17(4)	14.10(16)	0.04(2)	11.15(18)	0.18(4)	7.02(39)	n.a.	13.58(21)	3.14(8)	1.22(2)	93.27
			cpx HAl	7	43.82(41)	3.18(19)	9.36(61)	0.37(16)	4.26(14)	0.10(3)	13.14(22)	n.a.	23.36(18)	0.40(3)	0.01(2)	97.99
PU483	5	1100	gl	5	40.91(76)	4.42(16)	16.60(29)	0.02(2)	11.27(14)	0.23(5)	4.83(39)	n.a.	11.22(23)	3.98(14)	1.73(6)	95.21
			cpx HAl	4	44.08(1.00)	4.23(40)	11.24(81)	0.14(7)	4.92(23)	0.10(3)	12.04(55)	n.a.	23.13(20)	0.49(6)	0.02(2)	100.40
Picrobasalt runs																
P1151	10	1150	gl	11	47.75(36)	0.94(6)	16.22(30)	0.06(4)	8.19(26)	0.17(2)	9.39(11)	0.00(0)	11.40(8)	1.43(8)	0.53(1)	96.08
			cpx HAl	8	51.00(49)	0.48(10)	7.07(69)	1.19(12)	4.43(50)	0.12(2)	16.34(43)	0.00(0)	20.43(25)	0.29(2)	0.00(0)	101.35
P1180	10	1180	gl	10	47.44(71)	0.93(8)	16.31(56)	0.10(4)	8.31(34)	0.17(2)	9.15(52)	0.01(0)	12.00(24)	1.48(6)	0.52(2)	96.41
			cpx HAl	9	50.56(45)	0.40(4)	5.76(51)	1.28(17)	4.20(31)	0.14(1)	16.46(10)	0.00(0)	20.76(14)	0.25(3)	0.00(1)	99.81
R3	10	1200	gl	31	49.08(60)	0.86(10)	16.82(1.15)	0.02(5)	7.17(32)	0.08(7)	9.47(1.36)	0.00(0)	10.25(65)	1.77(28)	1.38(14)	96.90
			cpx HAl	7	50.29(46)	0.41(5)	7.33(24)	0.71(3)	4.52(9)	0.12(1)	16.88(45)	0.00(1)	18.77(55)	0.32(2)	0.01(1)	99.36

a more straightforward formulation that gives pressure as a function of atomic fractions:

$$P(\text{kbar}) = 771.48 + 4.956 \cdot Al_T - 28.756 \cdot Fe^{2+}_{M1} - 5.345 \cdot Fe^{3+} + 56.904 \cdot Al_{M1} + 1.848 \cdot Ti + 14.827 \cdot Cr - 773.74 \cdot Ca - 736.57 \cdot Na - 754.81 \cdot Mg_{M2} - 763.20 \cdot Fe^{2+}_{M2} - 759.66 \cdot Mn - 1.185(Mg_{M2})^2 - 1.876 \cdot (Fe^{2+}_{M2})^2 \quad (2)$$

where, following the same treatment as in Nimis (1995):

$$(Fe^{2+}_{M1} \cdot Mg_{M2}/(Fe^{2+}_{M2} \cdot Mg_{M1}) = \exp(0.238 \cdot R^{3+} + 0.289 \cdot CNM - 2.315);$$

$$CNM = Ca + Na + Mn;$$

$$R^{3+} = Al_{M1} + Fe^{3+} + Ti + Cr;$$

$$Al_{M1} = Al_{tot} - Al_T;$$

$$Al_T = (2 - Si).$$

Equation 2 is useful in the absence of X-ray diffraction data, although Eq. 1 is preferable because of the higher precision of direct structural measurements relative to that of structure simulations, which are also affected by uncertainties of chemical analyses. Care should be taken that Fe^{3+} be not neglected and atomic fractions be normalized to 4.000 (see above) before substituting them into Eq. 2.

Compared with the earlier version, the new geobarometer shows remarkably better statistics in terms of both $P_{cal} - P_{exp}$ residuals and number of data. In the V_{cell} vs V_{M1} plot, the geobarometric grids calculated from the two versions appear not to differ much (Fig. 2). The revised geobarometer will give similar values for $P < 10$ kbar and slightly higher (up to ca. 2.5 kbar) values for $P > 10$ kbar. The overall standard deviation on P reproduction is reasonably low ($\sigma = 1.75$ kbar), although a few residuals are still unsatisfactorily high (Fig. 3). Moreover, compared to the anhydrous barometric grid, clinopyroxenes from water-bearing experiments are systematically shifted to markedly higher V_{cell} and V_{M1} (Fig. 2). This results in underestimation of pressure by ca. 1 kbar per 1 wt% H_2O in the melt (Fig. 4a). Therefore, Eqs. 1 and 2 are strictly applicable to essentially anhydrous magmatic systems. These shortcomings will be addressed in the following section.

An expanded solution for anhydrous and hydrous magmas

As stated above, V_{cell} and V_{M1} do not reflect the true unit-cell and site volumes of the clinopyroxene at the P-T conditions of crystallization. Especially for the unit-cell volume, which is actually an expression for the molar volume of the mineral phase, this approximation may constitute an over-simplification. Therefore, the unit-cell volumes calculated by structure modeling were corrected for thermal expansivity and compressibility by using the algorithm of Berman (1988):

$$\frac{\overline{V}_{P,T}}{\overline{V}_0} = 1 + v_1(P - P_0) + v_2(P - P_0)^2 + v_3(T - T_0) + v_4(T - T_0)^2 \quad . \quad (3)$$

Coefficients v_i for diopside (Di), hedenbergite (Hd), clinoenstatite (Cen), Ca-Tschermak's (Ct), esseneite, Al-buffonite, and jadeite end-members were assumed to be equivalent to those reported in Sack and Ghiorso (1994). Those for acmite (Ac) and CrCt (i.e. $CaCrAlSiO_6$) were assumed to be equivalent to those of jadeite and Ct, respectively. Coefficients for clinoferrosilite (Cfs) were taken to be consistent with the relation:

$$v_i^{Cfs} = v_i^{Hd} - v_i^{Di} + v_i^{Cen} \quad . \quad (4)$$

This choice implies that Mg_{M2} and Fe^{2+}_{M2} behave identically in the M2 site with respect to bulk thermal expansivity and compressibility. An alternate possibility was to assume the stoichiometric relation:

$$v_i^{Cfs} = 2v_i^{Hd} - 2v_i^{Di} + v_i^{Cen} \quad . \quad (5)$$

Equation 4 was preferred because it more properly accounts for location of Mg and Fe^{2+} cations on non-equivalent M1 and M2 sites. End-member fractions (X_j) were calculated according to Lindsley and Andersen (1983). The values of v_i were then calculated as $v_i = \sum_j v_{i,j} \cdot X_j$ and utilized for estimation of the corrected unit-cell volume (V^{corr}_{cell}) through Eq. 3.

As for the M1 polyhedron, the mean linear polyhedral thermal expansion coefficient can be expressed as a function of the Pauling bond strength (Hazen and Prewitt 1977):

$$\bar{\alpha} = 32.9(0.75 - z_c/n) \cdot 10^{-6}\,^{\circ}\text{C}^{-1} \quad , \quad (6)$$

where z_c is the mean cation valence, and n is the coordination number ($=6$). Equation 6 was calibrated between 20 and 1000 °C, but we assumed it to be valid over the whole range of experimental temperatures (1050 °C < T < 1430 °C). Assuming isotropic expansion, the change in volume with temperature for the M1 polyhedron is given by:

$$\Delta^T_{v_{M1}} = V^0_{M1}\left(\frac{2 + 3\bar{\alpha}(T - 25\,^{\circ}\text{C})}{2 - 3\bar{\alpha}(T - 25\,^{\circ}\text{C})} - 1\right) \quad . \quad (7)$$

The V^0_{M1} at 25 °C, 1 atm is that obtained by X-ray diffraction measurement or structure modeling (Nimis 1995), while $\bar{\alpha}$ is calculated through Eq. 6. The mean polyhedral bulk modulus (K) is expressed (Hazen and Finger 1982) as:

$$K = \frac{z_c}{d^3} \cdot 7500(\text{kbar}) \quad , \quad (8)$$

where d is the M1 cation-oxygen mean bond distance in Å. d can be calculated from modeled V_{M1} through the empirical relation:

$$d = 1.4133 + 0.05601 \cdot V_{M1} \quad (R^2 = 0.998) \quad . \quad (9)$$

Equation 9 is the result of a regression conducted over 409 $C2/c$ pyroxenes studied at the Dipartimento di Mineralogia e Petrologia, University of Padua (Dal Negro et al., work in preparation). Assuming isotropic

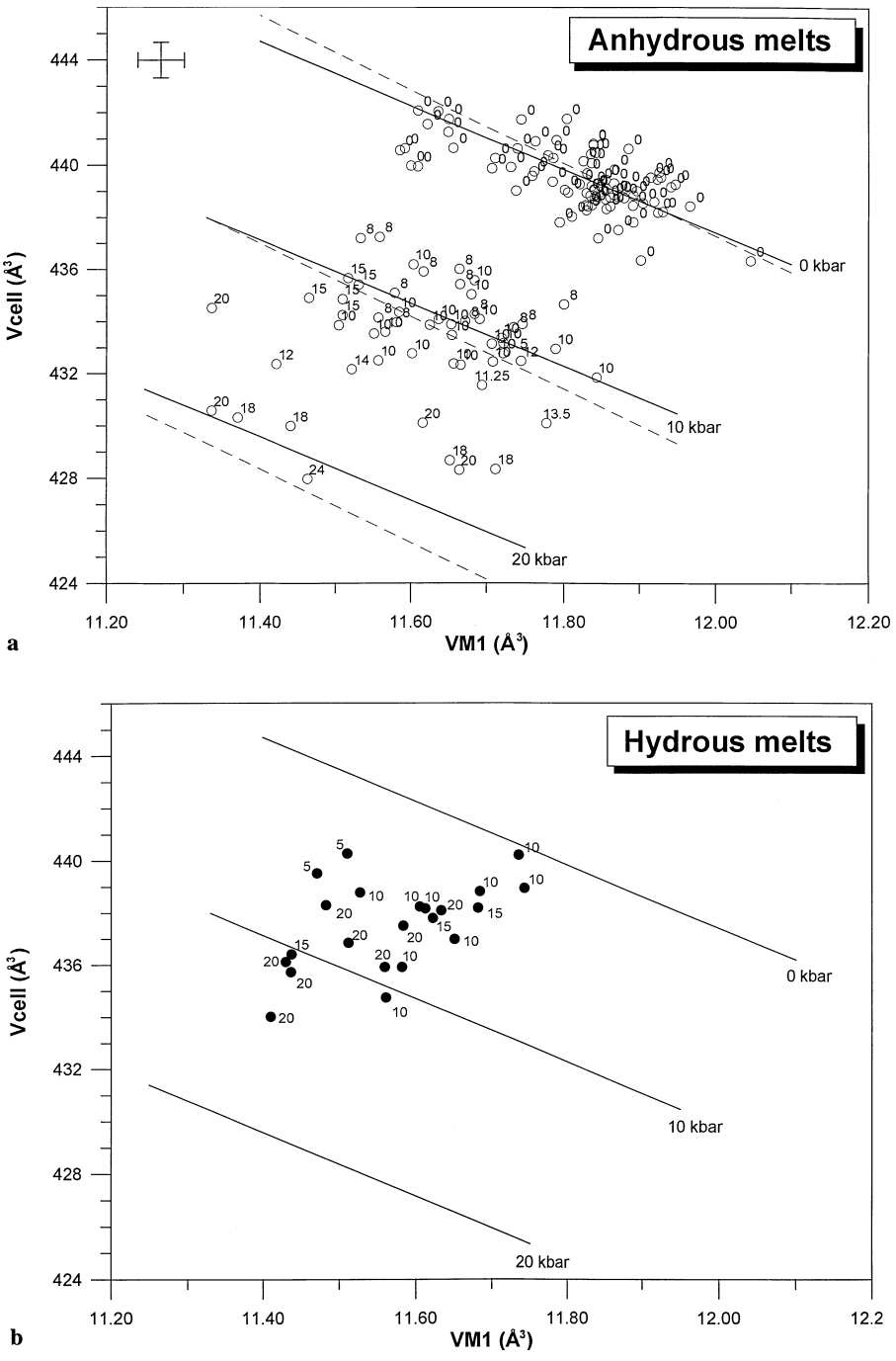

Fig. 2 **a** V_{cell} vs V_{M1} structural geobarometer for clinopyroxene from basic anhydrous magmas. The related empirical barometric grid obtained by linear regression is shown as *solid lines*. *Dashed lines* are the earlier barometric grid proposed by Nimis (1995). Numbers are nominal experimental pressures (kbar). Error bars are 1σ uncertainties of structure simulation (excluding propagation of errors of chemical analyses). Clinopyroxenes from hydrous experiments not utilized for calibration are shown for comparison in (**b**). Source of experimental data: **a** Baker and Eggler (1987; 4), Baker and Stolper (1994; 5), Bartels et al. (1991; 2), Bertolo et al. (1994; 1), Draper and Johnston (1992; 1), Dunn (1987; 4), Falloon and Green (1987; 7), Falloon and Green (1988; 4), Falloon et al. (1997; 2), Fujii and Bougault (1983; 1), Green and Ringwood (1967; 2 reanalysed; D.H. Green pers. comm.), Grove and Bryan (1983; 9), Grove et al. (1990; 7), Juster et al. (1989; 7), Kennedy et al. (1990; 7), Kinzler and Grove (1985; 1), Mahood and Baker (1986; 8), Meen (1990; 3), Putirka et al. (1996; 8), Sack and Carmichael (1984; 3), Sack and Ghiorso (1994; 1), Sack et al. (1987; 10), Stolper (1980; 1), Takahashi (1980; 1), Thompson (1974; 4), Thy (1991; 4), Toplis and Carrol (1995; 2), Tormey et al. (1987; 5), Walker et al. (1979; 7), Yang et al. (1996; 13), this work (Table 2; 1). **b** Adam and Green (1995; 7), this work (Table 2; 15). Numbers after semicolon in the above list are numbers of data points

compressibility and $P^0 \approx 0$ kbar, the change in volume with pressure for the M1 polyhedron is given by:

$$\Delta^P_{V_{M1}} = V^0_{M1}\left(\frac{2K-P}{2K+P}-1\right) \quad . \tag{10}$$

Finally, the corrected volume of the M1 polyhedron at *P-T* is:

$$V^{corr}_{M1} = V^0_{M1} + \Delta^T_{V_{M1}} + \Delta^P_{V_{M1}} \quad . \tag{11}$$

Within the considered *P-T* range, for both unit-cell and M1-polyhedron the most important contributions are those related to thermal expansivity.

The results of this treatment are illustrated in Figs. 3b and 5. The final geobarometric formulation is:

$$P = 654.47(\pm 13.11) - 1.189(\pm 0.039)\cdot V^{corr}_{cell} - 9.140(\pm 0.957)\cdot V^{corr}_{M1}$$
$$(\sigma = 1.70 \text{ kbar; max. dev.} = 5.4 \text{ kbar; R} = 0.971) \quad . \tag{12}$$

Higher-order regressions did not improve the fit.

The most important issue is that if thermal expansivity and compressibility are considered, the simple relation between unit-cell and M1-polyhedron volumes and pressure is maintained over the whole data set, including hydrous experiments. Moreover, most of the data that showed high, negative $P_{cal} - P_{exp}$ residuals

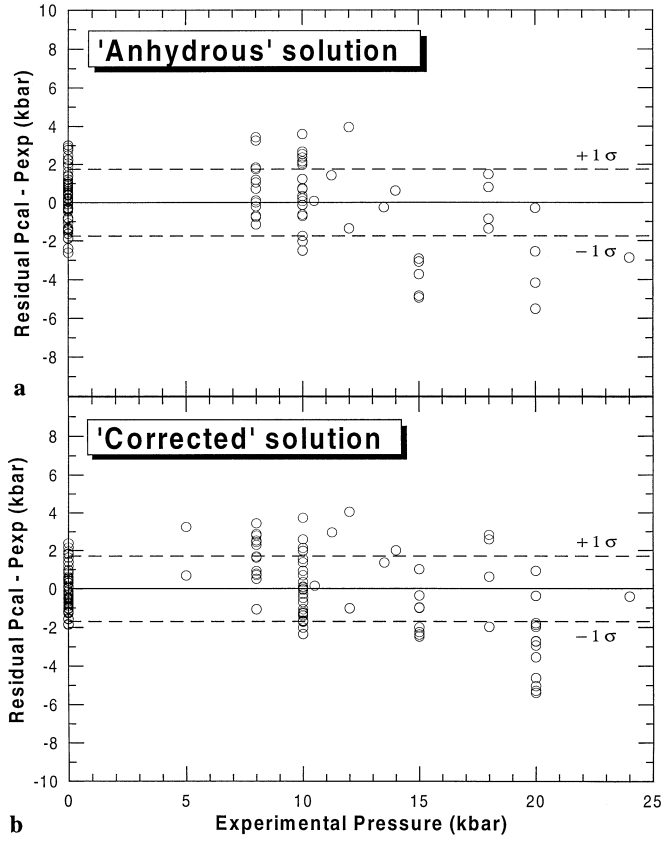

Fig. 3 $P_{cal} - P_{exp}$ residuals from regressions based on simplified anhydrous solution (Fig. 2a; Eq. 1) and corrected solution (Fig. 5; Eq. 12)

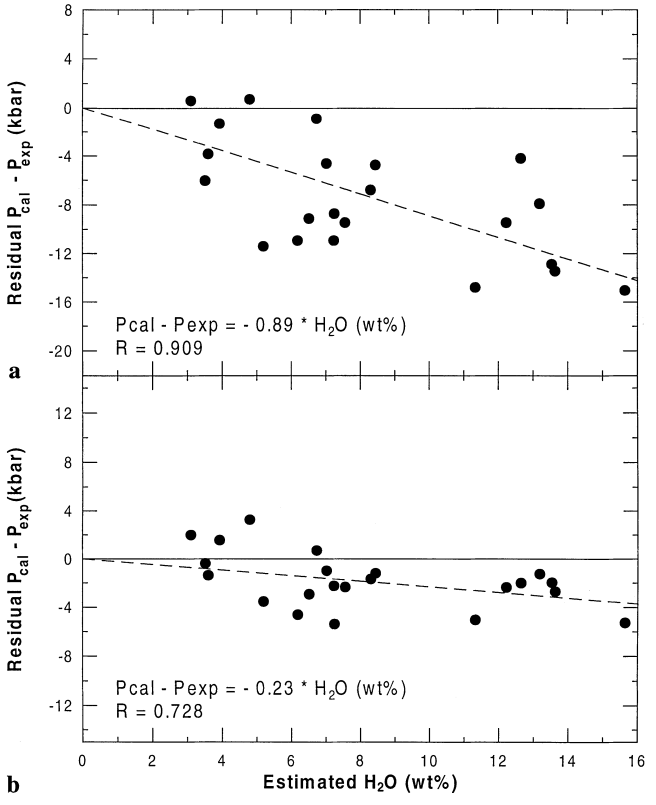

Fig. 4a, b Effect of water content on $P_{cal} - P_{exp}$ residuals for clinopyroxenes from hydrous experiments obtained using: **a** simplified anhydrous solution (Fig. 2a; Eq. 1); **b** corrected solution (Fig. 5; Eq. 12). Water contents of the coexisting melts were approximately calculated as 100 - Σ(oxides wt%). Linear best fit curves through origin are shown as *dashed lines*. The dependency of residuals on water content is apparent in **a** and virtually eliminated in **b**

based on the simplified *anhydrous* formulation (Fig. 2a), are fitted better by the *corrected* solution. Note that these data refer to experiments conducted at the lowest temperatures for a specific value of pressure. The low temperatures typical of hydrous experiments is also inferred to be the source of their high, negative residuals (Figs. 2b, 4a). Their good fit in the *corrected* formulation (Fig. 4b) suggests that water has negligible effects on pressure estimates. Variations of f_{O_2} do not affect the reproducibility of experimental pressures, nor does the presence of solid phases other than clinopyroxene (e.g. olivine, plagioclase, spinel, low-Ca pyroxenes, amphibole) in the equilibrium assemblage, save the above mentioned notable exceptions of garnet and melilite. Corrections for compressibility and thermal expansivity were not sufficient to reconcile clinopyroxenes from high-alumina basalts (Bartels et al. 1991; Delano 1977; Ulmer 1989; Putirka et al. 1996) with the bulk of the data.

Residuals from regression analysis are uniformly distributed over the considered pressure range, except for experiments at 20 kbar, most of which gave underestimated P values (Fig. 3b). These high residuals may reflect either poor-quality clinopyroxene data (disequilibrium or poor analyses) or inconsistency of the model. The thermobarometers of Putirka et al. (1996), which are based on the exchange of jadeite and Ca-Tschermak's components between clinopyroxene and melt over a wide compositional range, can be used to test the quality of these experimental data. The experiments that produced the highest residuals (>3.5 kbar) with the *anhydrous* and *corrected* calibrations are summarized in Table 3. It is worth noting that, excepting the two experiments of Dunn (1987), all the experiments at $P \geq 15$ kbar that were poorly reproduced by the present clinopyroxene geobarometers are also in bad agreement with Putirka et al.'s (1996) P-T estimates. Although we may not exclude the possibility that both methods fail to take into account all the possible compositional effects and may yield erroneous estimates for certain bulk compositions, this exercise suggests that the quality of experimental data may be a major source of error and the apparent dependency of $P_{cal} - P_{exp}$ residuals on P_{exp} (Fig. 3a, b) may be an artifact.

In practice, use of Eq. 12 requires knowledge of T and an approximate indication of P. The latter can initially be retrieved through Eq. 1 or 2 and then used as first input value in a trial-and-error procedure. As for T, an independent estimate (e.g. by pyroxene-solvus geothermometry) may be unavailable or poorly constrained.

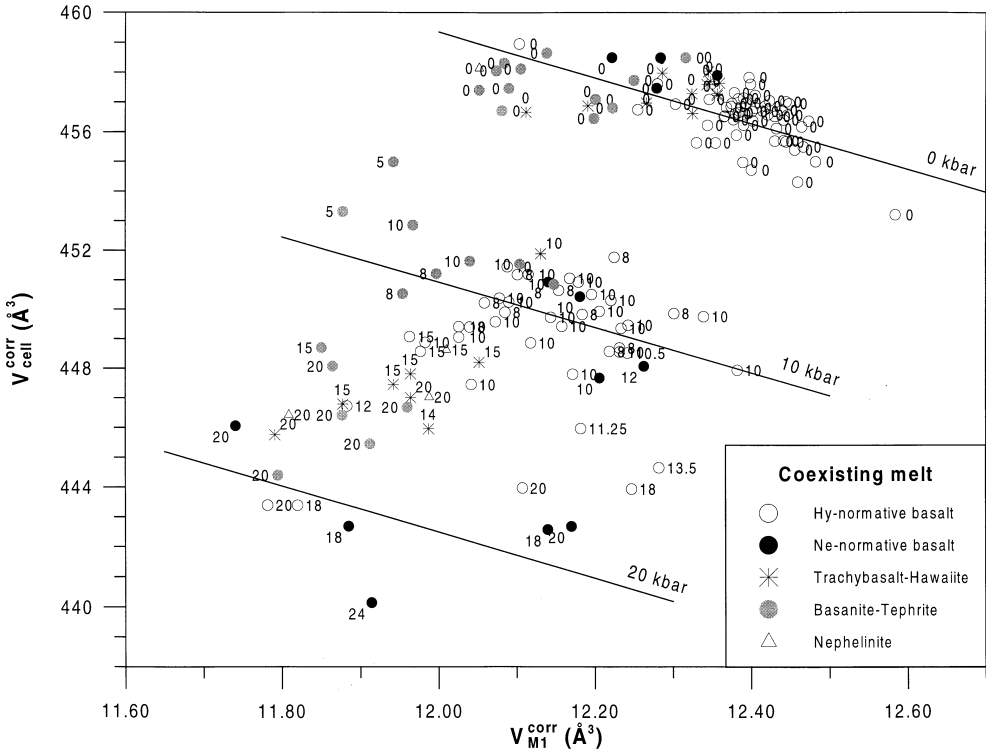

Fig. 5 Clinopyroxene structural geobarometer for anhydrous to hydrous basic magmas. V_{cell} and V_{M1} were corrected for thermal expansivity and compressibility (see text). Source of experimental data as in Fig. 2

In this case, propagation of uncertainties on T will strongly bias pressure estimates. This problem must be carefully considered, since the calculated P will rise by ca. 1 kbar per 20 °C underestimation of T.

To facilitate application of the present model, the geobarometer is implemented as a MS-DOS® or UNIX® software program (CpxBar)[4] designed to allow the pressure of crystallization to be retrieved directly from a major-oxide chemical analysis or from uncorrected unit-cell and M1-polyhedron volume X-ray data.

An application: geobarometry of ultramafic to gabbroic plutonic rocks of the southern Adamello batholith

In order to test the applicability of the proposed clinopyroxene geobarometer to hydrous calc-alkaline plutonic rocks, we have studied the clinopyroxene bearing ultramafic to gabbroic rocks of the southern Adamello batholith. This plutonic rock series is particularly well suited for rigorous testing of the geobarometer: (i) two contrasting, clinopyroxene-bearing plutonic series, ranging from ultramafic to intermediate (tonalitic) in composition occur in a restricted area (Bianchi and Dal Piaz 1937; Callegari and Dal Piaz 1973; Ulmer et al. 1983; Blundy and Sparks 1992); (ii) experimental data, obtained from a picrobasaltic dike (Ulmer 1989) occurring in the same area, provide independent constraints for the P-T evolution of this rock association.

One series of plutonic rocks, occurring at the southern border of the Tertiary calc-alkaline Adamello batholith, forms a plutonic body of approximately 3 km in diameter. It is called Val Fredda (VF) pluton and is composed predominantly (>80%) of biotite – leucotonalite. Coexisting mafic magmas produced a variety of ultramafic to mafic gabbroic rocks, ranging from olivine-two-pyroxene-hornblendites to clinopyroxene-hornblende gabbros and hornblende-gabbros. The pressure at the time of intrusion (42 Ma ago; Del Moro et al. 1983; Hansmann and Oberli 1991) is estimated to approximately 2–3 kbar, basing on geobarometry of the contact metamorphic country rocks (Riklin 1983) and the sedimentary overburden at the time of intrusion (Brack 1983). The particularity of this ultramafic – mafic rock association is the very early amphibole crystallization, the delayed plagioclase crystallization and the occurrence of enstatitic orthopyroxene, coexisting with clinopyroxene and pargasitic amphibole in the hornblendites (ultramafics). The pyroxene-bearing gabbros show a succession of early Al- and Cr-rich clinopyroxene, enclosed as corroded grains in amphibole phenocrysts (cumulus phases) in a matrix formed by strongly zoned plagioclase (An_{90} – An_{40}) and zoned low-Al clinopyroxene. The succession of crystallization is ol + Cr-sp (picotite) → cpx_1 → amph + opx → plag + cpx_2.

Phase equilibria studies on a primitive, parental composition (Ulmer 1989) picrobasalt with 2.6 wt% H_2O, produced coprecipitation of the cpx +

[4]CpxBar is written in Microsoft® Fortran and is available from WWW at 'http://dmp.unipd.it'.

Table 3 Highest $P_{cal} - P_{exp}$ residuals (> 3.5 kbar) from the *anhydrous* and *corrected* calibrations compared with Putirka et al.'s (1996) *P-T* estimates

Reference	#Run	Coex. melt[a]	*P*(kbar)	*T*(°C)	DP1[b]	DT2[b]	DT4[b]	DPanh[c]	DPcorr[c]
Draper and Johnston 1992	DPI21	Basalt (hy_N)	10	1250	0.6	−2	−28	3.6	3.7
Putirka et al. 1996	MA-11	Basalt (hy_N)	12	1275	2.4	1	−41	4.0	4.1
Meen 1990	A	Hawaiite	15	1200	−3.2[d]	116[d]	103[d]	−3.7	−0.4
Meen 1990	A	Hawaiite	15	1225	−2.8[d]	77[d]	63[d]	−4.8	−2.0
Dunn 1987	118a	Basalt (hy_N)	15	1265	0.4	−11	−34	−4.9	−2.5
Dunn 1987	119a	Basalt (ne_N)	20	1290	−1.3	3	−18	−5.5	−1.9
Putirka et al. 1996	A-6	Basalt (hy_N)	20	1390	2.9[d]	−17	−66[d]	−4.2	−2.7
Adam and Green 1995	1518	Trachybasalt	20	1100	−2.7	239[d]	–	–	−5.0
Adam and Green 1995	1534	Basanite	20	1200	−1.2	148[d]	138[d]	–	−4.6
This work	PU371	Basanite	20	1300	7.0[d]	101[d]	102[d]	–	−5.4
This work	PU376	Nephelinite	20	1100	3.2[d]	252[d]	267[d]	–	−5.3

[a] According to LeMaitre et al.'s (1989) classification
[b] Calc. – expt. residuals using Putirka et al.'s (1996) P1 barometer and T2 and T4 thermometers
[c] Calc. – expt. residuals from regressions of *anhydrous* and *corrected* clinopyroxene barometers (this work)
[d] Residual higher than 2σ

opx + amph paragenesis at conditions of 7–10 kbar and temperatures 1000–1050 °C (Fig. 6). This is in accordance with two-pyroxene geothermometry, which yielded temperatures of 980–1030 °C. The succession of $cpx_1 \rightarrow amph \rightarrow cpx_2$ + plag is interpreted as the result of a polybaric crystallization starting at high pressures (8–10 kbar) succeeded by low-pressure crystallization at the emplacement level of 2–3 kbar and temperatures around 900 °C. The results of clinopyroxene geobarometry, using Eq. 12 and natural clinopyroxene compositions (Table 4), are presented on Fig. 6 and Table 5. The barometry confirms the high-pressure (7–10 kbar) coprecipitation of cpx + opx + amph (samples GM1A and GM2A) and the low-pressure (0–4 kbar) crystallization of cpx + plag ($An_{90} - An_{40}$) for the Val Fredda plutonic rocks.

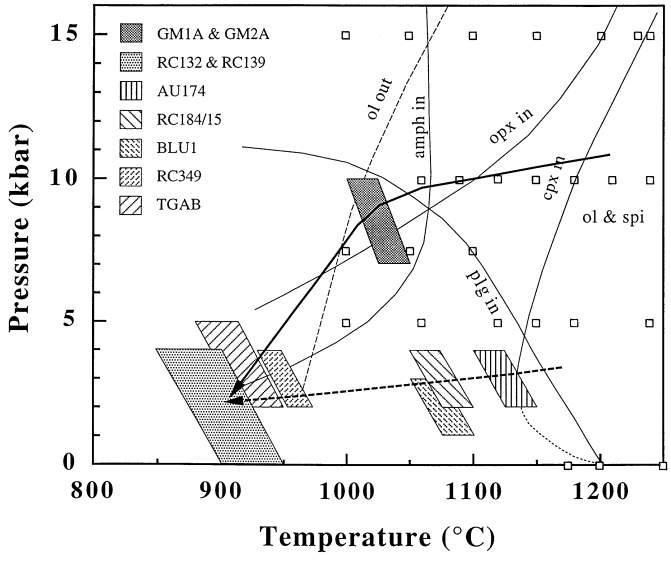

Fig. 6 Pressure-temperature diagram showing the results of clinopyroxene geobarometry using Eq. 12 applied to the southern Adamello ultramafic-mafic plutonic rocks. The *small open squares* and the *fine lines* display the result of phase equilibria experiments performed on a picrobasaltic composition from the same area (Ulmer 1989). The *P-T* path obtained for the two different rock series (Val Fredda pluton, *solid line with arrow*; and Blumone pluton, *broken line with arrow*) are consistent with petrographic and experimental results; the plutonics of the Val Fredda pluton exhibit an initial crystallization at intermediate crustal levels (25–30 km) with subsequent emplacement in shallow level and the final crystallization of the matrix clinopyroxene, while in contrast, the ultramafic-mafic rocks of the Blumone pluton show a shallow crystallization from ultrabasic (cumulate) rocks to intermediate qtz-diorites

The second ultramafic – mafic plutonic rock association forms a layered intrusion with subvertical layering, called the Blumone pluton (Ulmer et al 1983). High-temperature contact metamorphism (Ulmer 1982) in excess of 800 °C (monticellite-spinel) is in accordance with the interpretation of the gabbroic complex as derived from in situ crystallization of mafic magmas in shallow environment (2–3 kbar), most probably in feeder dikes. The older, stratified mafic complex (ranging from ol-gabbros to anorthosites) is intruded by slightly younger (not resolvable by zircon age dating, Hansmann and Oberli 1991) pyroxene-bearing qtz-gabbroic to tonalitic intrusions. Ultramafic rocks occur exclusively as inclusions in the contact zone between older stratified gabbros and the younger qtz-gabbroic to tonalitic intrusions. They consist of plagioclase-wehrlites (with cumulate textures) exhibiting variable amount of late amphibole overgrowth. The basic rock association of the Blumone pluton shows a different crystallization sequence from that described above for the Val Fredda pluton: ol + Cr-sp → cpx + plag + mgt → amph. Clearly amphibole is late crystallizing and plagioclase is an early phase, coprecipitating with the clinopyroxene. The plagioclase in the gabbroic rocks is extremely anorthitic ($An_{90} - An_{94}$), which is best explained by high H_2O-activity (Sisson and Grove 1993). Delayed amphibole crystallization and early plagioclase saturation, therefore, are not an effect of low H_2O-activity, but of low-pressure conditions during crystallization of the primocrysts. Field observations, petrography and experimental constraints (Ulmer 1989) consistently indicate a low pressure crystallization of all plutonic rocks of the Blumone unit starting from a primitive calc-alkaline basaltic to picritic magma.

Table 4 Temperature estimates and results of clinopyroxene barometry using Eq. 12. The temperature estimates are based on: (i) single and two-pyroxene thermometry, using the geothermometers of Brey and Köhler (1990) (Ca-in-opx, two-pyroxene solvus), the single-cpx geothermometer of Kretz (1982), and the solvus geothermometers of Wood and Banno (1973) and Wells (1977). The pressures for the thermometers were assumed 8 kbar for the Val Fredda hornblendites and 3 kbar for all other rocks; (ii) experimental phase relations and mineral chemistry, determined for a hydrous calc-alkaline picrobasalt from the southern Adamello (Ulmer 1989) in the *P-T* range 1 bar to 15 kbar and 900–1350 °C

Sample #	*T* (°C) (pyx-solvus)	*T* (°C) (experimental)	*P* (kbar) (CpxBar)
Val Fredda ultramafic-mafic rocks			
GM1A (opx-cpx-ol-hornblendite)	1000–1030	1000–1050	8–10
GM2A (opx-cpx-ol-hornblendite)	980–1020	1000–1050	7–9
RC139 (cpx-amph-gabbro)		850–950	0–4
RC132 (cpx-amph-gabbro)		850–900	1–4
Blumone ultramafic-mafic rocks			
AU174 (sp-plag-wherlite)		1100–1150	2–4
RC184/15 (plag-wherlite)		1050–1100	2–4
BLU1 (ol-gabbro)		1050–1100	1–3
RC349 (mgt-pyroxenite)	930–970		2–4
TGAB (opx-cpx-amph-diorite)	880–950		2–5

Table 5 Representative clinopyroxene analyses, used for the calculation of pressures listed on Table 4. Analyses were made with an ARL SEMQ and Cameca SX50 electron microprobe. Analytical conditions were 15 keV and 20 nA beam current; corrections were made using ZAF and PAP correction procedure; silicate and oxide standards have been used for calibration

Sample	GM1A	GM2A	RC132	RC139	AU174	RC184/15	BLU1	RC349	TGAB
SiO_2	49.57	50.98	52.58	52.57	49.35	51.27	49.99	52.23	52.69
TiO_2	0.83	0.64	0.11	0.09	0.90	0.42	0.88	0.23	0.19
Al_2O_3	6.05	4.27	1.24	1.18	5.88	3.80	4.48	1.31	1.06
Cr_2O_3	0.62	0.49	0.07	0.00	0.43	0.74	0.00	0.00	0.00
FeO	5.09	4.61	8.63	8.37	5.19	4.17	5.82	8.32	7.84
MnO	0.15	0.11	0.18	0.33	0.08	0.13	0.21	0.71	1.02
MgO	13.80	15.29	12.60	12.94	14.43	15.23	15.05	14.87	14.67
CaO	23.29	23.29	23.28	23.81	23.69	23.77	23.30	21.21	22.14
Na_2O	0.22	0.18	0.38	0.37	0.26	0.22	0.18	0.30	0.28
K_2O	0.01	0.00	0.00	0.01	0.00	0.00	0.00	0.00	0.00
Sum	99.63	99.87	99.06	99.68	100.20	99.75	99.90	99.18	99.88
Crystal-chemical partitionings (Papike et al. 1974)									
Si	1.833	1.872	1.983	1.968	1.809	1.884	1.839	1.953	1.958
Ti	0.023	0.018	0.003	0.003	0.025	0.012	0.024	0.007	0.005
Al	0.264	0.185	0.055	0.052	0.256	0.165	0.196	0.058	0.047
Cr	0.018	0.014	0.002	0.000	0.013	0.022	0.000	0.000	0.000
Fe^{3+}	0.021	0.034	0.000	0.033	0.084	0.038	0.092	0.045	0.047
Fe^{2+}	0.136	0.107	0.272	0.229	0.075	0.090	0.087	0.215	0.197
Mn	0.005	0.004	0.006	0.011	0.003	0.004	0.007	0.023	0.032
Mg	0.761	0.837	0.708	0.722	0.789	0.834	0.825	0.829	0.813
Ca	0.923	0.916	0.941	0.955	0.931	0.936	0.918	0.850	0.882
Na	0.016	0.013	0.027	0.027	0.019	0.016	0.013	0.022	0.020
Mg[a]	0.848	0.886	0.722	0.759	0.913	0.903	0.904	0.794	0.805
Σ Cations	4.000	4.000	3.999	4.000	4.000	4.000	4.000	4.000	4.000

[a] $Mg = Mg/(Mg + Fe^{2+})$

The results of the clinopyroxene geobarometry, listed in Table 4, and illustrated in Fig. 6, show consistently low pressures (1–5 kbar) for all clinopyroxene-bearing rock types investigated. The high-temperature rocks (ultramafics and gabbroic cumulates) do not contain orthopyroxene (in accordance with the phase diagram, see Fig. 6). Therefore, the temperature of clinopyroxene crystallization were estimated from phase relations. The clinopyroxene barometry is clearly consistent with the petrologic and experimental constraints.

The results obtained with the proposed clinopyroxene geobarometer (Eq. 12) for the southern Adamello ultramafic to gabbroic rocks, clearly demonstrate the applicability of this new geobarometric tool. The system investigated, hydrous calc-alkaline rocks, does normally not permit the determination of crystallization pressures other than by phase equilibria constraints. An important restriction for the application of this geobarometer is its sensitivity with respect to temperature. In order to apply the barometer to hydrous magmatic systems, the temperature of clinopyroxene crystallization has to be known or estimated quite accurately (e.g. within ± 50 °C).

Discussion and concluding remarks

The linear dependency of unit-cell and M1-site volumes of magmatic $C2/c$ pyroxene on the pressure of crystallization is confirmed by a large population of data over a wide range of geologically relevant physico-chemical conditions. Regression statistics are improved if the field of melt compositions is extended from subalkaline basalts to nephelinites and both dry and hydrous magmatic systems are included, provided structural data are corrected for thermal expansivity and compressibility.

The existence of a simple relation between P and clinopyroxene composition, expressed in terms of structural parameters, is not inconsistent with Duhem's theorem. First, in the special situation of a melt that begins to crystallize at depth, T is not totally independent, because it is constrained by the position of the liquidus curve in the P-T-X space. As long as the melt stays *basic* in composition, T cannot vary strongly. Second, if the main variations in bulk chemistry concern the degree of silica saturation or the content of CaO, as in most natural basic magmas, compositional effects are entirely taken up by the inverse, linear V_{cell} vs V_{M1} correlation that can be observed at any P (Fig. 5). This is particularly evident along the 0-kbar isobar, where a more complete set of melt compositions is represented. Going from subalkaline, quartz-normative basalts to progressively more silica-undersaturated types of melt, the composition of the clinopyroxene changes significantly, but the resulting structural trend is easily predictable. The effects of a decrease of a_{SiO_2} (or an increase of a_{CaO}) can approximately be described by the exchange $Mg_{M2}Mg_{M1}(Si_T)_{1+x} \rightarrow Ca_{M2}(Ti_x,Fe^{3+},Al)_{M1}(Al_T)_{1+x}$. Such exchange induces opposite effects on V_{cell} and V_{M1} (V_{cell} increases and V_{M1} decreases), hence the bias on pressure estimate tends to cancel out. Similar crystal chemical constraints possibly also compensate the effects of reactions with mineral phases competing with clinopyroxene for Ca or Al, such as plagioclase or low-Ca pyroxenes.

Despite the fact that relations between P and clinopyroxene chemistry are *not* simple (cf. Thompson 1974) the structural parameters V_{cell} and V_{M1} exhibit simple relations with P. The present geobarometers based on P-V_{cell} − V_{M1} systematics are applicable to a wide range of natural clinopyroxene-bearing basic and ultrabasic igneous rocks. They are expected to give the most useful results for well-preserved, cumulitic products, like those represented by pyroxenitic xenoliths and megacrysts. In principle, they should also be applicable to mantle equilibrium partial-melting residua, provided these did not re-equilibrate after melt extraction. In any case, clinopyroxenes that re-equilibrated after magmatic crystallization or melting during subsolidus processes are unsuitable for geobarometric purposes, unless their primary composition can be recovered (e.g. by integrated analysis of exsolution structures; Nimis 1998).

Although the present work is believed to be an important step in clinopyroxene geobarometry, the expanded formulations proposed here can probably be improved in the future. We believe one of the most important pitfalls to be the fact that strategies behind existing experimental works have almost invariably been aimed at best defining the equilibrium composition of the melt. The reproducibility of clinopyroxene composition has seldom been sought. Further, the selection of *true* equilibrium composition from chemically heterogeneous crystals has often been neglected in favor of grand averages of spurious analyses. Moreover, most existing data refer to experiments at 1 atm. In particular, data in the range $0 < P < 8$ kbar are still scarce and the 20-kbar isobar is poorly bracketed, therefore further experimental work at these pressure conditions is demanded. Compositional effects, like those induced by changes in aluminum activity, deserve to be studied in detail. An assessment of the geobarometric potential of clinopyroxene in more evolved magmatic systems will be presented in a subsequent paper.

Acknowledgements We are indebted to TJ Falloon for supplying unpublished microprobe data and for precious suggestions. We are also thankful to A Dal Negro, J Ganguly, JAD Connoly, and G Ottonello for useful discussion. We thank V Trommsdorff for donation of the basanite starting material and numerous discussions on the genesis of the Austrian basanites. Comments and suggestions of two anonymous referees are gratefully appreciated. The financial support of the C.N.R. "Centro di Studio per la Geodinamica Alpina" (Padova) and of MURST grants is acknowledged.

References

Adam J, Green TH (1995) The effect of pressure and temperature on the partitioning of Ti, Sr and REE between amphibole, clinopyroxene and basanitic melts. Chem Geol 117: 219–233

Baker DR, Eggler DH (1987) Compositions of anhydrous and hydrous melts coexisting with plagioclase, augite, and olivine or low-Ca pyroxene from 1 atm to 8 kbar: application to the Aleutian volcanic center of Atka. Am Mineral 72: 12–28

Baker MB, Stolper EM (1994) Determining the composition of high-pressure mantle melts using diamond aggregates. Geochim Cosmochim Acta 58: 2811–2827

Bartels KS, Kinzler RJ, Grove TL (1991) High pressure phase relations of primitive high-alumina basalts from Medicine Lake volcano, northern California. Contrib Mineral Petrol 108: 253–270

Bellieni G, Piccirillo EM, Zanettin B (1981) Classification and nomenclature of basalts. IUGS Commission on Systematics of Igneous Rocks, Circ 34, Contr 87, Cambridge

Berman RG (1988) Internally-consistent thermodynamic data for minerals in the system Na_2O-K_2O-CaO-MgO-FeO-Fe_2O_3-Al_2O_3-SiO_2-TiO_2-H_2O-CO_2. J Petrol 29: 445–522

Bertolo S, Nimis P, Dal Negro A (1994) Low-Ca augite from experimental alkali basalt at 18 kbar: structural variation near the miscibility gap. Am Mineral 79: 668–674

Bianchi A, Dal Piaz Gb (1937) Il settore meridionale del massiccio dell'Adamello. Relazioni sul rilevamento e studi preliminari della zona compresa fra la Valle Stabio e l'alta Valle del Caffaro. Boll Uff Geol Ital 62: 1–87

Blundy JD, Sparks RSJ (1992) Petrogenesis of mafic inclusions in granitoids of the Adamello Massif, Italy. J Petrol 33: 1039–1104

Bohlen SR, Essene EJ, Boettcher AL (1980) Reinvestigation and application of olivine-qtz-orthopyroxene barometry. Earth Planet Sci Lett 47: 1–10

Bose K, Ganguly J (1995) Quartz-coesite transition revisited: reversed experimental determination at 500–1200 °C and retrieved thermochemical properties. Am Mineral 80: 231–238

Brack P (1983) Multiple intrusions – examples from the Adamello Batholith (Italy) and their significance on the mechanism of intrusion. Mem Soc Geol Ital 26: 145–157

Brey GP, Köhler T (1990) Geothermometry in four-phase lherzolites II. New thermobarometers, and practical assessment of existing thermobarometers. J Petrol 31: 1353–1378

Callegari E, Dal Piaz Gb (1973) Field relationship between the main igneous masses of the Adamello intrusive massif (Northern Italy). Mem Ist Geol Miner Univ Padova 29: 1–39

Delano JW (1977) Experimental melting relations of 63545, 76015, and 76055. Proc 8th Lunar Sci Conf: 2097–2123

De La Roche H, Leterrier J, Grandclaude P, Marchal M (1980) A classification of volcanic and plutonic rocks using R_1 and R_2 diagram and major element analysis: its relationships with current nomenclature. Chem Geol 29: 183–210

Del Moro A, Pardini G, Quercioli C, Villa IM, Callegari E (1983) Rb/Sr systematics on rocks from the Adamello batholith, Southern Alps. Mem Soc Geol Ital 26: 261–284

Draper DS, Johnston AD (1992) Anhydrous *PT* phase relations of an Aleutian high-MgO basalt: an investigation of the role of olivine-liquid reaction in the generation of arc-alumina basalts. Contrib Mineral Petrol 112: 501–519

Duncan AM, Preston RMP (1980) Chemical variation of clinopyroxene phenocrysts from the trachybasaltic lavas of Mount Etna, Sicily. Mineral Mag 43: 765–770

Dunn T (1987) Partitioning of Hf, Lu, Ti, and Mn between olivine, clinopyroxene and basaltic liquid. Contrib Mineral Petrol 96: 476–494

Ellis DJ (1976) High pressure cognate inclusions in the Newer Volcanics of Victoria. Contrib Mineral Petrol 58: 149–180

Falloon TJ, Green DH (1987) Anhydrous partial melting of MORB pyrolite and other peridotite compositions at 10 kbar: implications for the origin of primitive MORB glasses. Mineral Petrol 37: 181–219

Falloon TJ, Green DH (1988) Anhydrous partial melting of peridotite from 8 to 35 kb and the petrogenesis of MORB. J Petrol Spec Lithosphere Issue: 379–414

Falloon TJ, Green DH, O'Neill HStC, Hibberson WO (1997) Experimental tests of low degree peridotite partial melting compositions: implications for the nature of anhydrous near-solidus peridotite melts at 1 GPa. Earth Planet Sci Lett 152: 149–162

Fujii T, Bougault H (1983) Melting relations of a magnesian abyssal tholeiite and the origin of MORBs. Earth Planet Sci Lett 62: 283–295

Green DH, Ringwood AE (1967) The genesis of basaltic magmas. Contrib Mineral Petrol 15: 103–190

Grove TL, Bryan WB (1983) Fractionation of pyroxene-phyric MORB at low pressure: an experimental study. Contrib Mineral Petrol 84: 293–309

Grove TL, Kinzler RJ, Bryan WB (1990) Natural and experimental phase relations of lavas from Serocki volcano. Proc Ocean Drill Proj Sci Res 106/109: 9–17

Hansmann W, Oberli F (1991) Zircon inheritance in an igneous rock suite from the southern Adamello batholith (Italian Alps). Implications for petrogenesis. Contrib Mineral Petrol 107: 501–518

Hazen RM, Finger LW (1982) Comparative crystal chemistry. Temperature, pressure, composition and the variation of crystal structure. Wiley, Chichester

Hazen RM, Prewitt CT (1977) Effects of temperature and pressure on interatomic distances in oxygen-based minerals. Am Mineral 62: 309–315

Irving AJ (1980) Petrology and geochemistry of composite ultramafic xenoliths in alkalic basalts and implication for magmatic processes within the mantle. Am J Sci 280 A: 389–426

Johannes W, Chipman DW, Hays JF, Bell PM, Mao HK, Boettcher AL, Newton RC, Seiffert F (1971) An interlaboratory comparison of piston-cylinder pressure calibration using the albite breakdown reaction. Contrib Mineral Petrol 32: 24–38

Juster TC, Grove TL, Perfit MR (1989) Experimental constraints on the generation of FeTi basalts, andesites, and rhyodacites at the Galapagos spreading center, 85°W and 95°W. J Geophys Res 94: 9251–9274

Kennedy AK, Grove TL, Johnson RW (1990) Experimental and major element constraints on the evolution of lavas from Lihir Island, Papua New Guinea. Contrib Mineral Petrol 104: 722–734

Kinzler RJ, Grove TL (1985) Crystallization and differentiation of Archean komatiite lavas from northeast Ontario: phase equilibrium and kinetic studies. Am Mineral 70: 40–51

Knutson J, Green TH (1975) Experimental duplication of a high-pressure megacryst/cumulate assemblage in a near-saturated hawaiite. Contrib Mineral Petrol 52: 121–132

Kretz R (1982) Transfer and exchange equilibria in a portion of the pyroxene quadrilateral as deduced from natural and experimental data. Geochim Cosmochim Acta 46: 411–421.

Le Maitre RW, Bateman P, Dudek A, Keller J, Lameyre J, Le Bas MJ, Sabine PA, Schmid R, Sorensen H, Streckeisen A, Woolley AR (1989) A classification of igneous rocks and glossary of terms. Recommendation of the IUGS Subcommission on the Systematics of Igneous Rocks. Blackwell, Oxford

Lindsley DH, Andersen DJ (1983) A two-pyroxene thermometer. Proc 13th Lunar Planet Sci Conf. J Geophys Res Suppl 88: A887–A906

Mahood GA, Baker DR (1986) Experimental constraints on depths of fractionation of mildly alkalic basalts and associated felsic rocks: Pantelleria, Strait of Sicily. Contrib Mineral Petrol 93: 251–264

Meen JK (1990) Elevation of potassium content of basaltic magma by fractional crystallization: the effect of pressure. Contrib Mineral Petrol 104: 309–331

Nimis P (1995) A clinopyroxene geobarometer for basaltic systems based on crystal-structure modeling. Contrib Mineral Petrol 121: 115–125

Nimis P (1998) Clinopyroxene geobarometry of pyroxenitic xenoliths from Hyblean Plateau (SE Sicily, Italy). Eur J Mineral 10: 521–533

Papike JJ, Cameron K, Baldwin K (1974) Amphiboles and pyroxenes: characterization of other than quadrilateral components and estimates of ferric iron from microprobe data. Geol Soc Am Abstr Progr 6: 1053–1054.

Presnall DC, Brenner NL (1974) A method for studying iron silicate liquids under reducing conditions with negligible iron loss. Geochim Cosmochim Acta 38: 1785–1788

Putirka K, Johnson M, Kinzler R, Longhi J, Walker D (1996) Thermobarometry of mafic igneous rocks based on clinopyroxene-liquid equilibria, 0–30 kbar. Contrib Mineral Petrol 123: 92–108

Riklin K (1983) Contact metamorphism of the Permian red sandstones in the Adamello area. Mem Soc Geol Ital 26: 159–169

Sack RO, Carmichael ISE (1984) $Fe_2 \leftrightarrow Mg_2$ and $TiAl_2 \leftrightarrow MgSi_2$ exchange reactions between clinopyroxenes and silicate melts. Contrib Mineral Petrol 85: 103–115

Sack R, Ghiorso MS (1994) Thermodynamics of multicomponent pyroxenes: III. Calibration of $Fe^{2+}(Mg_{-1})$, $TiAl_2(MgSi_2)_{-1}$, $TiFe^{3+}(MgSi_2)_{-1}$, $AlFe^{3+}(MgSi)_{-1}$, $Al_2(MgSi)_{-1}$ and $Ca(Mg)_{-1}$ exchange reactions between pyroxenes and silicate melts. Contrib Mineral Petrol 118: 271–296

Sack RO, Walker D, Carmichael ISE (1987) Experimental petrology of alkalic lavas: constraints on cotectics of multiple saturation in natural basic liquids. Contrib Mineral Petrol 96: 1–23

Shannon RD (1976) Revised effective ionic radii and systematic studies of interatomic distances in halides and chalcogenides. Acta Crystallogr A32: 751–767

Sisson TW, Grove TL (1993) Experimental investigations of the role of H_2O in calc-alkaline differentiation and subduction zone magmatism. Contrib Mineral Petrol 113: 143–166

Stolper E (1980) A phase diagram for mid-ocean ridge basalts: preliminary results and implications for petrogenesis. Contrib Mineral Petrol 74: 13–27

Takahashi E (1980) Melting relations of an alkali-olivine basalt to 30 kbar, and their bearing on the origin of alkali basalt magmas. Carnegie Inst Washington Yearb 79: 271–276

Thompson RN (1974) Some high-pressure pyroxenes. Mineral Mag 39: 768–787

Thy P (1991) High and low pressure phase equilibria of a mildly alkalic lava from the 1965 Surtsey eruption: experimental results. Lithos 26: 223–243

Toplis MJ, Carrol MR (1995) An experimental study of the influence of oxygen fugacity on Fe-Ti oxide stability, phase relations, and mineral-melt equilibria in ferro-basaltic systems. J Petrol 36: 1137–1170

Tormey DR, Grove TL, Bryan WB (1987) Experimental petrology of normal MORB near the Kane Fracture Zone: 22°–25° N, mid-Atlantic ridge. Contrib Mineral Petrol 96: 121–139

Trommsdorff V, Dietrich V, Flisch M, Stille P, Ulmer P (1990) Mid-Cretaceous, primitive alkaline magmatism in the Northern Calcareous Alps: significance for Austroalpine geodynamics. Geol Rundsch 79: 85–97

Ulmer P (1982) Monticellite-clintonite bearing assemblages at the southern border of the Adamello-Massif. Rend Soc Ital Mineral Petrol 38: 617–628

Ulmer P (1986) Basische und ultrabasische Gesteine des Adamello (Provinzen Brescia und Trento, Norditalien). ETH Dissertation Nr. 8105, Zuerich

Ulmer P (1989) High pressure phase equilibria of a calc-alkaline picro-basalt: implications for the genesis of calc-alkaline magmas. Carnegie Inst Washington Yearb 88: 28–35

Ulmer P, Callegari E, Sonderegger UC (1983) Genesis of the mafic and ultramafic rocks and their genetical relations to the tonalitic-trondhjemitic granitoids of the Southern part of the Adamello Batholith (Northern Italy). Mem Soc Geol Ital 26: 171–222

Ulmer P, Trommsdorff V, Dietrich VJ (1989) The genesis of Cretaceous basanites from the Calcareous Alps (Austria): experimental, geochemical and field constraints. (abstract) IAVCEI Abstracts New Mexico Bur Mines Miner Resour Bull 131: 274

Walker D, Shibata T, DeLong SE (1979) Abyssal tholeiites from the Oceanographer Fracture Zone. Contrib Mineral Petrol 70: 111–125

Wells PRA (1977) Pyroxene thermometry in simple and complex systems. Contrib Mineral Petrol 62: 129–139

Wood BJ, Banno S (1973) Garnet-orthopyroxene and orthopyroxene-clinopyroxene relationships in simple and complex systems. Contrib Mineral Petrol 42: 109–124

Yang H-J, Kinzler RJ, Grove TL (1996) Experiments and models of anhydrous, basaltic olivine-plagioclase-augite saturated melts from 0.001 to 10 kbar. Contrib Mineral Petrol 124: 1–18